Electronic Supplementary Information

Nitrogen-doped PtSn Nanocatalyst Supported on Hollow Silica Sphere for Acetic Acid Hydrogenation

Jiahua Zhou,[a] Yujun Zhao,[a,*] Jian Zhang,[a] Yue Wang,[a] Oliver Y Gutiérrez,[b] Shengnian Wang,[c] Zhengxiang Li,[d] Peng Jin,[d,*] Shengping Wang,[a] Xinbin Ma,[a] Johannes Lercher[b,e]

[a.] Key Laboratory for Green Chemical Technology of Ministry of Education. Collaborative Innovation Center of Chemical Science and Engineering, School of Chemical Engineering and Technology, Tianjin University, Tianjin 300072, China.

[b.] Institute for Integrated Catalysis, Pacific Northwest National Laboratory, Richland, WA99352, US.

[c.] Institute for Micromanufacturing, Louisiana Tech University, Ruston, LA71272, US.

[d.] School of Materials Science and Engineering, Hebei University of technology, Tianjin 300130, China.

[e.] Department of Chemistry and Catalysis Research Center, TU München, Garching 85748, Germany.

*Correspondence concerning this article should be addressed to Y. Zhao at yujunzhao@tju.edu.cn or P. Jin at china.peng.jin@gmail.com, Tel.& fax: 022-87401818

1. Experimental

1.1 Materials

3-Aminopropyl triethoxysilane (APTES), Oleic acid (>90%), tin (II) chloride were purchased from Aladdin. $SnCl_2 \cdot 2H_2O$ (>98%) was purchased from Sinopharm Chemical Reagent Co., LTD. Ethanol was purchased from YuanLi Chemical Reagent Co., LTD. The platinum (II) tetra-ammine chloride ($[Pt(NH_3)_4]Cl_2$), Pt>55.4%) was purchased from Beijing HWRK Chem Co., LTD. Tetraethoxyorthosilicate (TEOS>99.5%) and ammonium hydroxide (NH_4OH) were purchased from Tianjin Kermel Chemical Co., LTD. All the reagents were used without further purification.

1.2 Preparation of Sn/NHSS

The N-doped Sn/HSS was prepared by O/W microemulsion-templated self-assembly method (one-pot method) induced by anionic surfactant. Firstly, 1.40 g of Oleic Acid (OA) was added into 140 mL of distillated water to form a uniform O/W emulsion. Then, $SnCl_2$ (0.03 g) was added into the above emulsion, followed by adding another mixture of TEOS (6.935 g) and APTES (1.10 g). The solution was vigorously stirred for approximately 5 min at room temperature. Then further aging for another 24 h was performed at 80 °C to ensure the formation of the nitrogen modified silica network with tin oxide. The initial molar composition of OA/APTES/TEOS/H_2O was 1:1:6.7:1600 and the Sn content was adjusted to be 1 wt.% (in the final solid) unless otherwise noted. The resulting precipitate was filtered and washed with deionized water several times to remove excess ions before drying in air at 105 °C for 12 h. The as-prepared support was calcined at 550 °C in air for 10 h.

1.3 Preparation of Sn/SiO_2-SG

Sn/SiO_2 (denoted as Sn/SiO_2-SG) in this work were prepared by sol-gel method. The molar ratio of TEOS: C_2H_5OH: H_2O was 1:3.85:10.20. TEOS was first mixed with ethanol and an alcoholic solution of $SnCl_2 \cdot 2H_2O$. Then, given amount of deionized water was added into the solution with vigorously stirring at room temperature and the pH of the resulted mixture was kept at *ca.* 4. The generated sol was aged for 24 h

at 60 °C. The precipitate was filtered and washed with ethanol until chloride ions could not be detected, and then dried at 105 °C. The obtained solid was finally calcined in air at 500 °C for 4 h.

1.4 Preparation Sn/N-SiO_2-SG

Amino-functionalized Sn/SiO_2-SG (designated as N-doped Sn/SiO_2-SG) was synthesized using 3-aminopropyl trimethoxysilane (APTES) as the N source.[1] Approximately 2 g Sn/SiO_2-SG support and 1 g APTES were well dispersed in 100 mL ethanol by stirring. The mixture was refluxed at 90 °C for 24 h, and the obtained solid was then collected by filtration, washed with ethanol for several times before drying at 60 °C. Finally, the solid was calcined at 500 °C in air for 4 h.

1.5 Preparation PtSn/NHSS catalyst

Supported Pt catalysts were prepared by depositing the metal precursor ($[Pt(NH_3)_4]$ Cl_2) onto the support by strong electrostatic adsorption (SEA) method.[2] The as-synthesized N-doped Sn/HSS supports were firstly suspended in NH_4OH solution (aq., pH=10.60) under stirring to get mixture A. Then the solution of $[Pt(NH_3)_4]Cl_2$ was added to mixture A with controlled concentration to obtain 0.5 wt. % Pt loading on the support. After the mixture was stirred for another 10 h, it was filtrated under vacuum and the resulted solid was washed with distilled water and dried at 105 °C for 5 h. The catalyst was denoted as PtSn/NHSS. For comparison, PtSn/SiO_2 and PtSn/N-SiO_2 were also prepared with the same method by using Sn/SiO_2-SG and Sn/N-SiO_2-SG as supports, respectively.

1.6 Catalytic performance test

Activity and selectivity measurements in gas-phase catalytic hydrogenation of acetic acid (AcOH) were carried out in a stainless-steel fixed-bed reactor with an internal diameter of 8 mm. About 0.65 g (40-60 mesh) were placed in the center of the reactor and both sides of the catalyst bed were packed with quarts powder (20-40mesh). Prior to the reaction, the catalyst was reduced with H_2 (99.999%, 100 ml·min^{-1}) at 300 °C for 4 h. Then AcOH (99.5%,) was pumped into the reactor system using a constant-flow pump and vaporized through a preheater. Catalytic test was performed

under 270 °C and 2.6 MPa with weight hourly space velocity (WHSV) of AcOH varing from 1 to 3 h^{-1}. The reaction products collected in the condenser were analyzed using a gas chromatograph (BEIFEN 3420A) with an HP-INNOWAX capillary column (30 m × 0.25 mm × 0.25 μm) and a flame ionization detector (FID). More than three samples were taken under the same experimental conditions and the results were averaged to ensure reproducibility. AcOH conversion was determined by carbon balance based on compounds in the liquid phase (equation 1), and the product selectivity were calculated based on the carbon-containing products (equation 2). Only the selectivity of EtOH and AcOEt were observed because other hydrogenation products like aldehyde could be neglected at the selected reaction conditions.

The turn over frequency (TOF) of the catalyst was measured under the conditions (T=270 °C, P=2.6 MPa, H_2/AcOH=20 (mol mol^{-1})). TOF_{Pt} was calculated as hourly converted reactant on per exposed Pt atom (equation 3). Specific activity of Pt was calculated as hourly consumed reactant divided by weight amount of actual loaded Pt (equation 4).

$$\text{Conversion}(\%)=\frac{\text{mol of AcOH put into the reactor - mol of AcOH put in the product}}{\text{mol of AcOH put into the reactor}}\times 100\% \quad (1)$$

$$\text{Selectivity}(\%)=\frac{\text{mol of EtOH or AcOEt in the product}}{\text{mol of AcOH put into the reactor - mol of AcOH in the product}}\times 100\% \quad (2)$$

$$TOF_{Pt}=\frac{WHSV_{AcOH}\times Conv\times MW_{Pt}}{Wt_{Pt}\times D_{Pt}\times MW_{AcOH}}(mol_{AcOH}\cdot mol_{Pt}^{-1}\cdot h^{-1}) \quad (3)$$

$$\text{Specific Activity}_{Pt}=\frac{F_{AcOH}\times Conv}{Wt_{Pt}\times m_{cat}}(g_{AcOH}\cdot g_{Pt}^{-1}\cdot h^{-1}) \quad (4)$$

$WHSV_{(AcOH)}$: the weight hourly space velocity of the reaction (h^{-1});

MW_{Pt}: the relative mass of Pt ($g\cdot mol^{-1}$);

Wt_{Pt}: the actual loading of Pt ($g_{Pt}\cdot g_{cat}^{-1}$);

D_{Pt}: dispersion obtained from TEM (%);

Conv: the conversion of AcOH (%);

MW_{AcOH}: the relative mass of AcOH ($g\cdot mol^{-1}$);

F_{AcOH}: flow rate of AcOH (g/min);

m_{cat}: the mass of the catalyst (g).

1.7 Catalyst Characterization

Textual properties of the samples were measured by a N_2-adsorption method using a Micromeritics Tristar II 3000 Analyser at 77 K. Pore size distribution was determined by the Barrett-Joyner-Halenda (BJH) method from the desorption branches of the adsorption isotherms, and the specific surface areas were calculated from the isotherms using the Brunauer-Emmett-Teller (BET) method.

The powder X-ray diffraction (XRD) characterization was performed on a Rigaku C/max-2500 diffractometer with a Cu Kα radiation (40 kV, 200 mA) (λ=0.15418 nm). The reduced catalyst was scanned at $5°\cdot min^{-1}$ from 10° to 90°.

Transmission electron microscope (TEM) was conducted at 100 kV using a Philips TECNAI G2 F20 system electron microscope equipped with a field emission gun. The samples were ultrasonically dispersed in ethanol and then the suspension was dropped onto a copper grid, followed by drying in air. About 300 particles were counted to evaluate the platinum particle size distribution.

Scanning electron microscope (SEM) was used to observe the morphology of the samples by employing a Hitachi S4800 field-emission microscope at 10.0 kV.

The elemental analysis of Pt and Sn of all samples were performed on an inductively coupled plasma optical emission spectroscopy (ICP-OES, VISTA-MPX, Varian). Before the measurement, about 100 mg of the sample was dissolved in HF aqueous solution, and excessive amount of boric acids solution were added to form a mixture.

Chemisorption measurements were performed on an AutoChem II 2920 (Micromeritics) in pulse mode using CO as the adsorbing gas and He as the carrier gas. The catalyst samples were reduced at 300 °C for 2 h in 10 vol.% H_2/Ar flow. Then the samples were cooled and purged with He for 60 min, followed by pulse dosing 10% CO/He of 20 ml/min, until apparent saturation (constancy in the peak area) occurred.

Hydrogen temperature-programmed reduction (H_2-TPR) was performed on an AutoChem II 2920 (Micromeritics) equipped with a TCD detector. About 100 mg of the fresh catalysts were pretreated in Ar flow at 200 °C for about 1 h, and then cooled to

60 °C. The TPR measurement was conducted by heating the catalysts to 600 °C with a temperature ramp of 10 °C·min^{-1} in a flow of 10 vol% H_2/Ar (30 mL·min^{-1}).

Zetasizer Nano (Malvern) was used to obtain the PZC values of the supports by measuring the zeta potentials of the supports.

Fourier transform infrared (FTIR) spectra of pyridine adsorption were collected on a Thermo Scientific Nicolet 6700 (32 scans, 4 cm^{-1}). The sample powders were prior reduced at 300 °C in H_2 for 4 h and then cooled to room temperature. After that, the powder was pressed into a self-supporting disk (ca.20 mg) under the pressure of 6 MPa before introduced into the IR cell. The disk was re-reduced in 10 vol.% H_2/Ar at 300 °C for 1 h, then, it was evacuated at the same temperature. After cooled to 150 °C, the samples were saturated with vapor pyridine for 0.5 h and then evacuated at 150 °C for 0.5 h. Spectra were recorded at the evacuation temperature in the range of 4000-650 cm^{-1}. The amount of Lewis acid sites in the samples were calculated by peak deconvolution of characteristic band at ca.1450 cm^{-1}.

1.8 Computational Details

All calculations were performed at the spin-polarized DFT level within the DMol^3 program[3, 4]. The Perdew, Burke and Ernzerhof (PBE)[5] exchange–correlation functional (with Tkatchenko and Scheffler's dispersion correction[6]) was used with the double numerical plus d-functions (DND) basis set. We used a reconstructed α-quartz (001) surface to represent the SiO_2 support.[7] The (3×3) supercell includes 4 Si atomic layers of SiO_2 and sampled with a 3 × 3 × 1 K-point grid. The slabs were separated by more than 20 Å of vacuum. The convergence criteria for the structure optimization and energy calculation were set to (a) a SCF tolerance of 1.0 × 10^{-5} eV/atom, (b) an energy tolerance of 2.0 × 10^{-5} Ha, (c) a maximum force tolerance of 0.004 Ha/Å, and (d) a maximum displacement tolerance of 5.0 × 10^{-3} Å. The adsorption energy (E_{ads}) is the energy of SiO_2 surface with the Pt cluster adsorbed to it minus the energy sum of the isolated SiO_2 surface and metal cluster.

References

[1] X. Zheng, H. Lin, J. Zheng, H. Ariga, K. Asakura and Y. Yuan, *Top. Catal.*, 2014, **57**, 1015-1025.

[2] G. Xu, J. Zhang, S. Wang, Y. Zhao and X. Ma, *RSC Adv.*, 2016, **6**, 51005-51013.

[3] B. Delley, *J. Chem. Phys.*, 1990, **92**, 508-517.

[4] B. Delley, *J. Chem. Phys.*, 2000, **113**, 7756-7764.

[5] J. Perdew, K. Burke and M. Ernzerhof, *Phys. Rev. Lett.*, 1996, **77**, 3865-3868.

[6] A. Tkatchenko and M. Scheffler, *Phys. Rev. Lett.*, 2009, **102**, 073005.

[7] T.P. Goumans, A. Wander, W. Brown and C. Catlow, *Phys. Chem. Chem. Phys.*, 2007, **9**, 2146-2152.

[8] S. Zhang, Z.Q. Huang, Y. Ma, W. Gao, J. Li, F. Cao, L. Li, C. Chang and Y. Qu, *Nat. Commun.*, 2017, **8**, 15266.

[9] C. Yu, H. Xu, Q. Ge and W. Li, *J. Mol. Catal. A:Chem.*, 2007, **266**, 80-87.

[10] K. Cheng, M. Virginie, V. Ordomsky, C. Cordier, P. Chernavskii, M. Ivantsov, S. Paul, Y. Wang, A. and Khodakov, *J. Catal.*, 2015, **328**, 139-150.

Figure Captions

Fig. S1 (a) N_2 adsorption-desorption isotherms; (b) BJH pore size distribution spectrum of catalysts；

Fig. S2 XRD patterns of various reduced catalysts.

Fig. S3 SEM images of the reduced samples (a), (c) 0.5Pt1Sn/SiO_2; (b), (d) 0.5Pt1Sn/N-SiO_2.

Fig. S4 TEM images and EDS mapping images of 0.5Pt1Sn/N-SiO_2 catalyst.

Fig. S5 FTIR spectra of chemisorbed pyridine on reduced catalysts.

Fig. S6 The most stable sites for Pt_4 clusters adsorption on SiO_2 and NHSS supports.

Fig. S7 (a) Total density of state of Pt/SiO_2; (b) Partial density of state of Pt/SiO_2; (c) Total density of state of Pt/NHSS; (d) Partial density of state of Pt/NHSS.

Fig. S8 Plots of charge density difference for the Pt/NHSS and Pt/SiO_2 catalysts. (a), (e) Side and top views of density isosurface slice across the N sites of Pt/NHSS; (b), (f) Side and top views of density isosurface slice across the Pt sites of Pt/NHSS; (c), (g) Side and top views of density isosurface slice across the O sites of Pt/SiO_2; (d), (h) Side and top views of density isosurface slice across the Pt sites of Pt/SiO_2. The electron-density isosurfaces are plotted at 0.01 e $bohr^{-3}$. The color bar represents the change of electron density compared with the isolated Pt cluster and NHSS or SiO_2(red: excess; blue: depletion).

Fig. S9 H_2-TPR profiles over the catalysts: (a) 0.5Pt1Sn/SiO_2, (b) 0.5Pt1Sn/NHSS.

Fig. S10 Actual zeta potential versus adsorption pH (pH_f) plot for Sn/SiO_2 (PZC=1.1), Sn/N-SiO_2 (PZC=1.2) and Sn/NHSS (PZC=2.08).

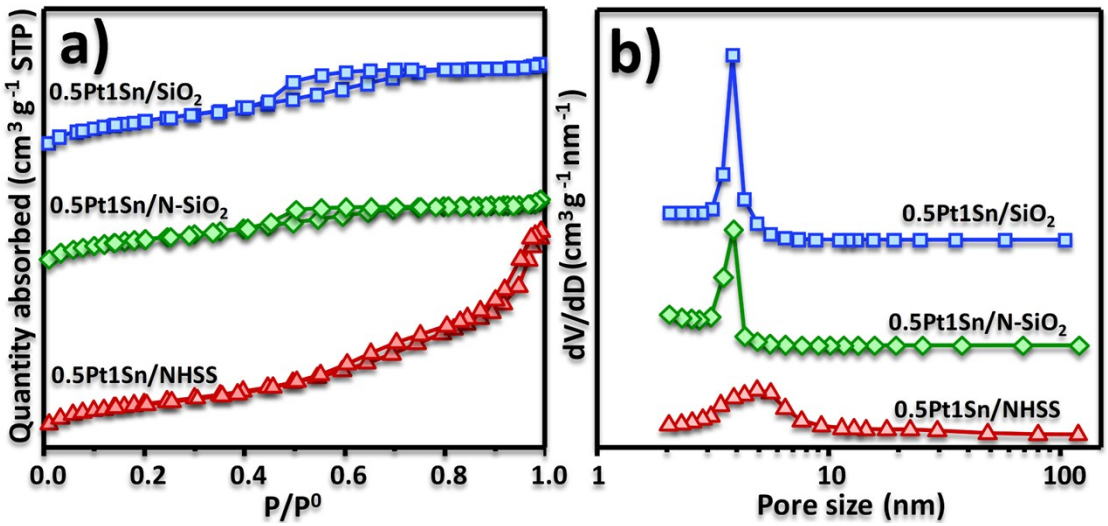

Fig. S1 (a) N_2 adsorption-desorption isotherms; (b) BJH pore size distribution spectrum of catalysts.

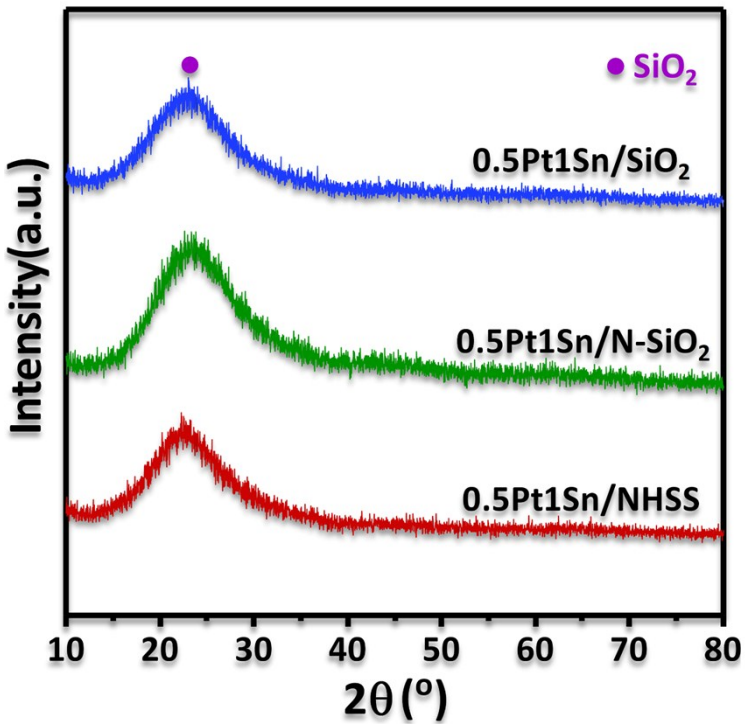

Fig. S2 XRD patterns of various reduced catalysts.

For all the reduced catalysts, the XRD patterns (Fig. S2) only showed one broad peak originated from 15° to 35°, which was attributed to the reflection peaks of the SiO_2 frameworks. No any characteristic peak of Sn species can be observed in the XRD patterns for all the samples, indicating that Sn species were highly distributed on the surface of catalysts.

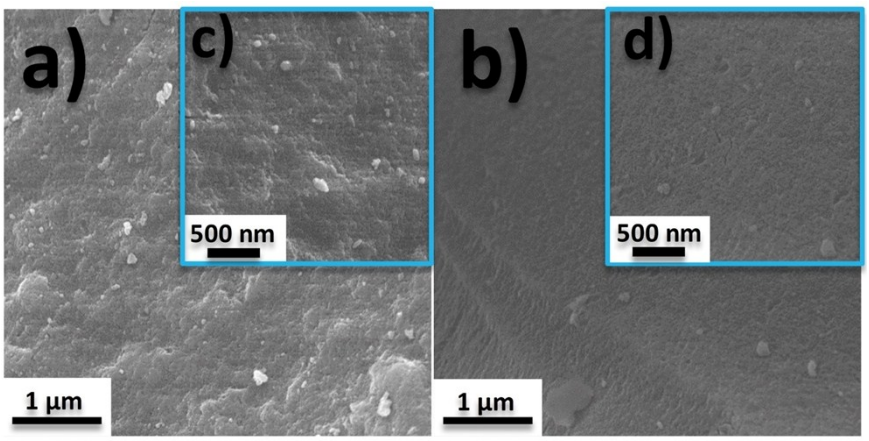

Fig. S3 SEM images of the reduced samples (a), (c) 0.5Pt1Sn/SiO_2, (b), (d) 0.5Pt1Sn/N-SiO_2.

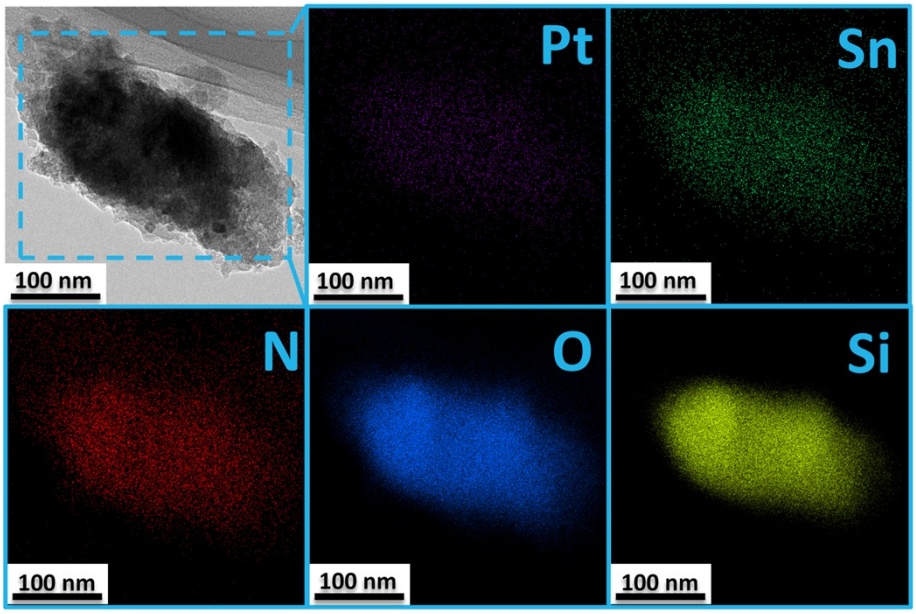

Fig. S4 TEM images and EDS mapping images of 0.5Pt1Sn/N-SiO_2 catalyst.

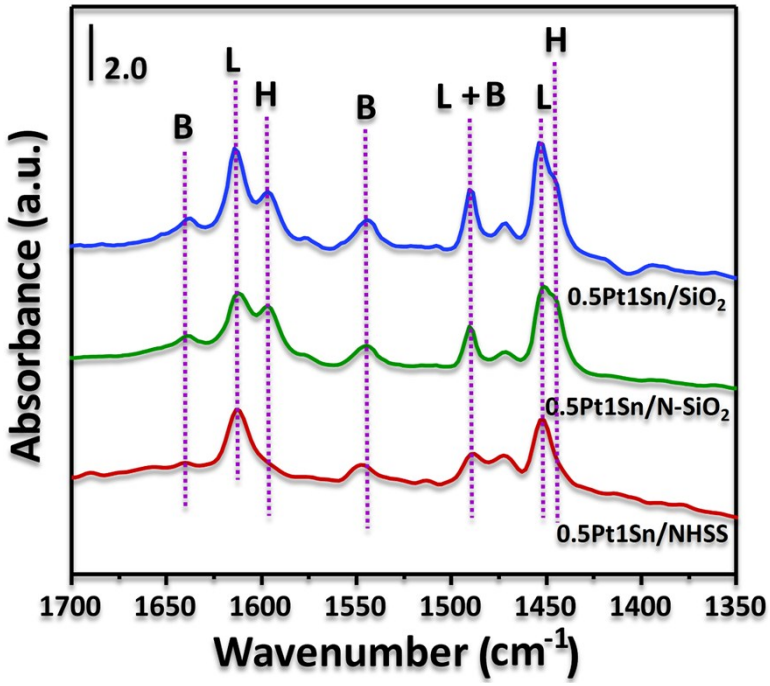

Fig. S5 FTIR spectra of chemisorbed pyridine on reduced catalysts.

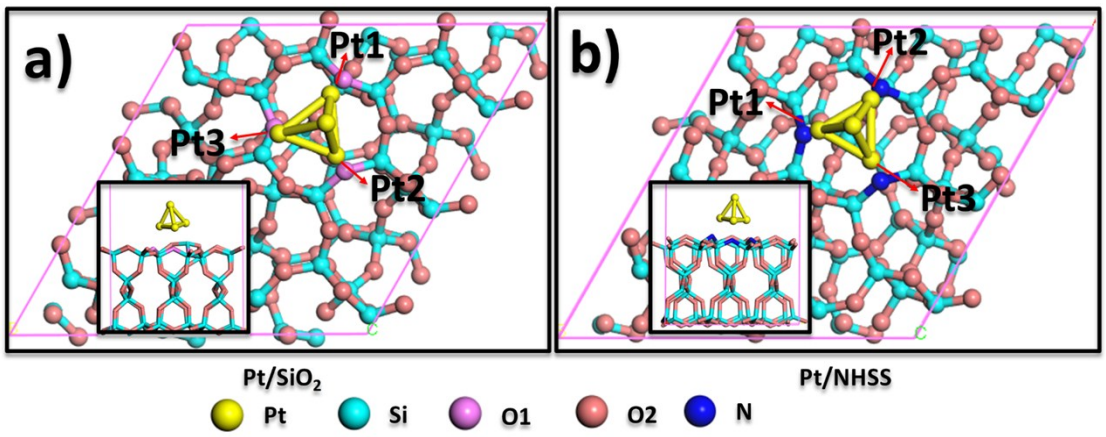

Fig. S6 The most stable sites for Pt_4 clusters adsorption on SiO_2 and NHSS supports (insets are the side views).

In the second model, O1 was replaced by N on basis of the assumption that N was doped into the SiO_2 structure.

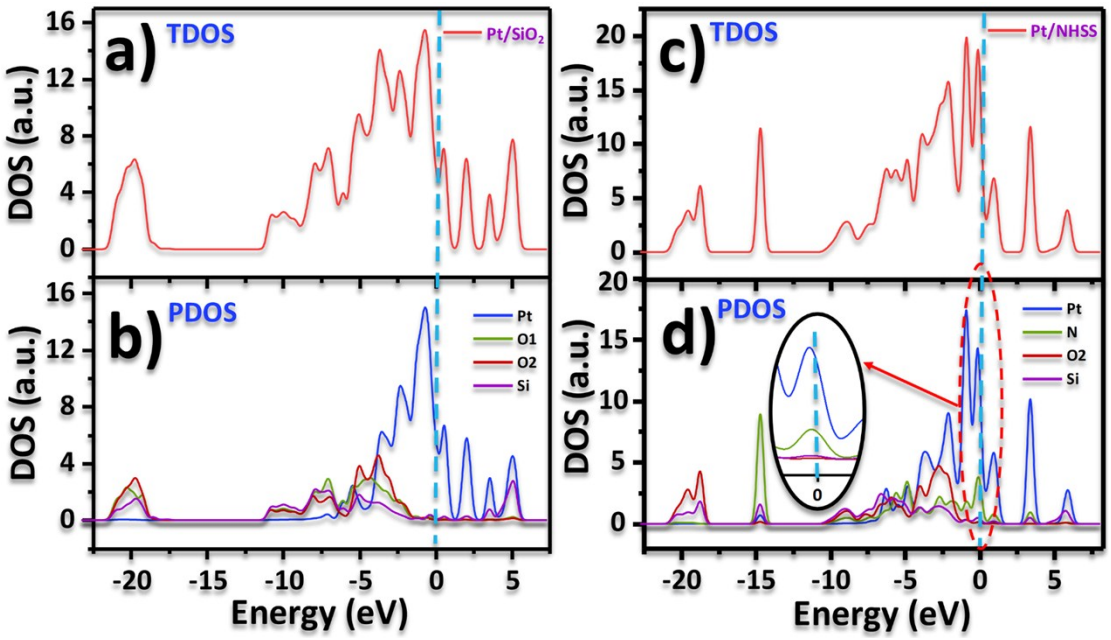

Fig. S7 (a) Total density of state of Pt/SiO_2; (b) partial density of state of Pt/SiO_2; (c) total density of state of Pt/NHSS; (d) partial density of state of Pt/NHSS. The dashed straight lines denote the Fermi level at 0 eV.

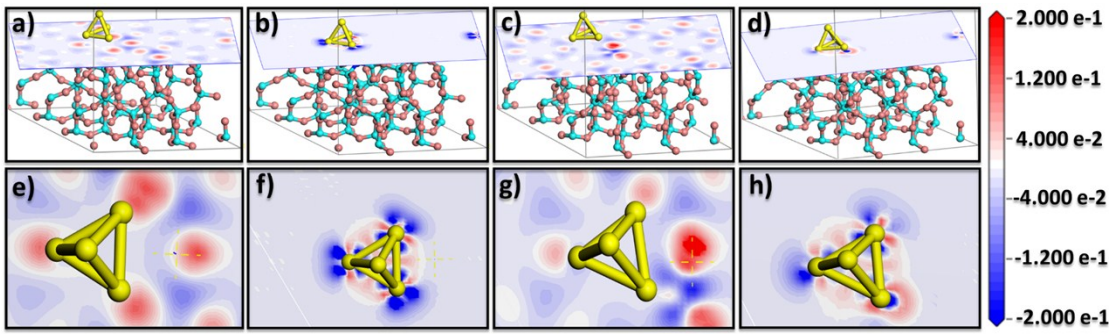

Fig. S8 Plots of charge density difference for the Pt/NHSS and Pt/SiO_2 catalysts. (a), (e) Side and top views of density isosurface slice across the N sites of Pt/NHSS; (b), (f) Side and top views of density isosurface slice across the Pt sites of Pt/NHSS; (c), (g) Side and top views of density isosurface slice across the O sites of Pt/SiO_2; (d), (h) Side and top views of density isosurface slice across the Pt sites of Pt/SiO_2. The electron-density isosurfaces are plotted at 0.01 e $bohr^{-3}$. The color bar represents the change of electron density compared with the isolated Pt cluster and NHSS or SiO_2(red: excess; blue: depletion).

To further clear the N effect on Pt, charge density difference[8] calculated by DFT method were used to verify the electronic effects of N dopant on Pt and study the interactions between Pt and different supports. Based on the stable adsorption configurations for both Pt/SiO_2 and Pt/NHSS (Fig. S6), the charge density difference (Fig. S8 (a), (b), (c), (d)) showed that Pt donated electron to N, which led to the formation of more electron-deficient Pt species induced probably by the stronger interaction between Pt and N. In addition, compared with Pt/SiO_2 (Fig. S8 (h)), Pt/NHSS showed a color of deeper blue in Fig. S8 (f), which can further illustrate that Pt at the interface was in a state of electron-deficient due to the strong interaction between Pt and N.

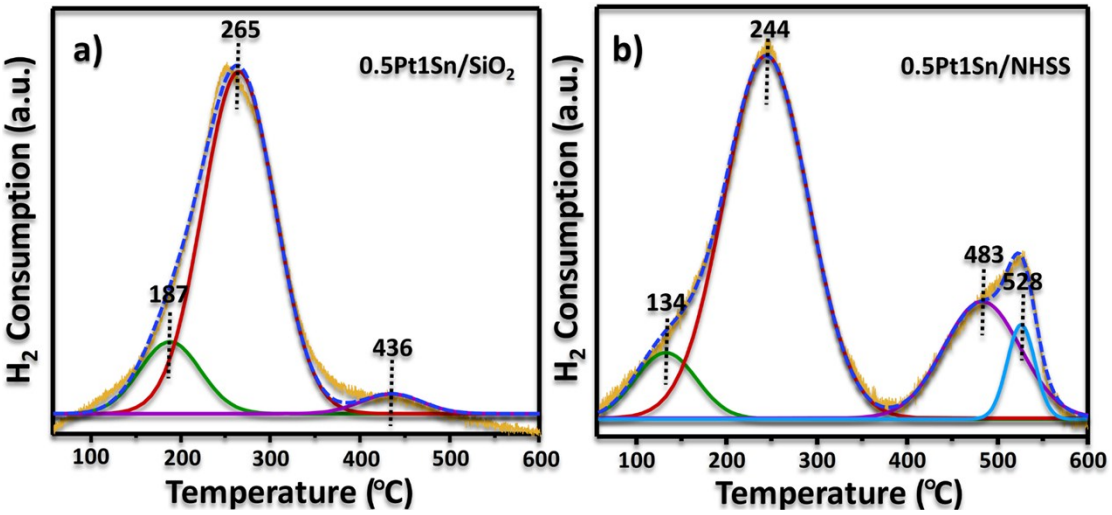

Fig. S9 H_2-TPR profiles over the catalysts: (a) 0.5Pt1Sn/SiO_2, (b) 0.5Pt1Sn/NHSS.

H_2-TPR was also used to illustrate the interaction between Pt and N. As shown in Fig. S9, the catalysts presented several peaks with increasing reduction temperature, which were attributed to the different interactions between Pt species and the supports. It is noteworthy that there was a small peak at low temperature of around 130-190 °C, which could be attributed to the weak interaction between Pt and the support. It is obvious that most of the Pt species were reduced at around 200-300 °C for 0.5Pt1Sn/SiO_2 and 0.5Pt1Sn/NHSS catalyst, which was assigned to the reduction of Pt-(O-Sn≡)$_y^{2-y}$ species.[9] However, part of Pt species was reduced at higher temperature (around 483 °C) for 0.5Pt1Sn/NHSS catalyst, which could be attributed to the reduction of Pt species having strong interaction with N. It was generally accepted that the stronger interaction at the interface will lead to the formation of the smaller metal nanoparticles, which can be reduced more difficultly than larger one.[10] Therefore, the smaller Pt particles on the reduced PtSn/NHSS catalyst could be due to the strong interaction between Pt and N dopant. The reduction peak at 436 ^oC for 0.5Pt1Sn/SiO_2 was ascribed to be the reduction of SnO_2,[2] while the reduction temperature at 528 ^oC for PtSn/NHSS catalyst was suggested to be the reduction of the SnO_2 having strong interaction with N dopant.

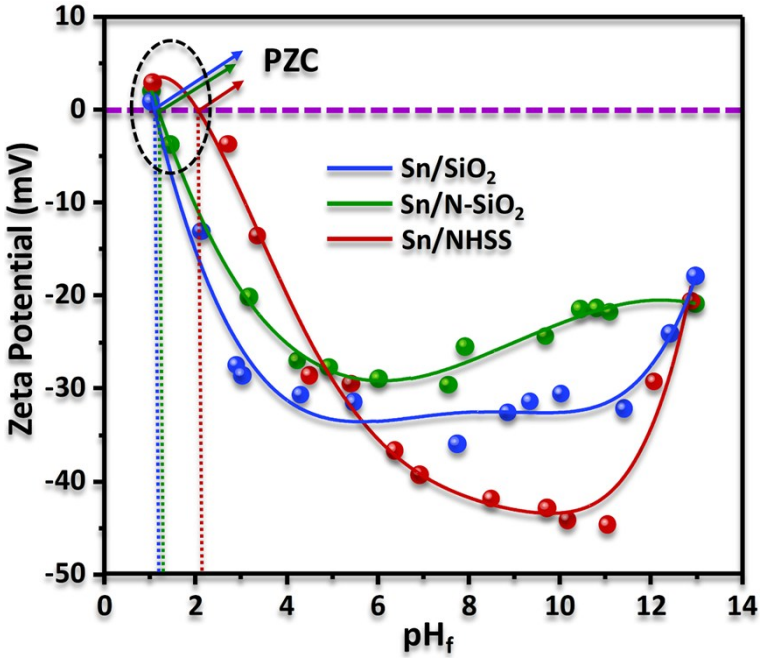

Fig. S10 Actual zeta potential versus adsorption pH (pH_f) plot for Sn/SiO_2 (PZC=1.1), $Sn/N\text{-}SiO_2$ (PZC=1.2) and Sn/NHSS (PZC=2.08).

As shown in Fig. S10, all the samples have the similar PZC value of about 1-2. It is noteworthy that only a small amount of APTES was used during the catalysts preparation, so that the PZC can be hardly affected. In the experiment, the pH of the solution was kept at 10.60, which was much higher than their respective PZC values. Therefore, the negative surface potentials on the supports ensured the adsorption of cationic $[Pt(NH_3)_4]^{2+}$.

Regarding the higher Pt loading of $PtSn/N\text{-}SiO_2$ than the nominal loading (Table 1) indicated in the experimental section, a loss of Sn/SiO_2 support was unexpected found during the pre-treatment process. The leaching of the SiO_2 (about 20 wt.%) happened during the reflux at 90 °C in the solution of APTES and ethanol. Therefore, the actual Pt loading was higher than the nominal content since the amount of the $[Pt(NH_3)_4]Cl_2$ solution was kept at the same level as other samples during the Pt loading process.

Table S1 Catalytic performance of catalysts. Reaction conditions: P=2.6 MPa, T=270 °C, H_2/AcOH=20.

Catalyst	WHSV = 1 h^{-1}			WHSV = 2 h^{-1}			WHSV = 3 h^{-1}		
	Conv.	EtOH	AcOEt	Conv.	EtOH	AcOEt	Conv.	EtOH	AcOEt
0.5Pt1Sn/SiO_2	68.2	71.8	26.4	49.1	83.3	14.9	34.0	87.0	11.0
0.5Pt1Sn/N-SiO_2	79.6	78.6	20.3	56.1	85.2	13.3	41.3	89.3	9.0
0.5Pt1Sn/NHSS	86.6	90.0	9.0	67.1	90.7	7.3	45.6	91.9	6.7

Table S2 The calculated adsorption energies (E_{ads}) and the bonding length (d) for the most stable Pt_4 adsorption on SiO_2 (Pt-O) and NHSS (Pt-N) supports shown in Fig. S6

Adsorption model	E_{ads}(eV)	d (Å)	d_{min}[a] (Å)	d_{avg}[b] (Å)
Pt/SiO_2 (Pt-O)	-1.26	2.26 (Pt1) 2.34 (Pt2) 3.08 (Pt3)	2.26	2.56
Pt/NHSS (Pt-N)	-3.22	2.02 (Pt1) 2.02 (Pt2) 2.04 (Pt3)	2.02	2.03

[a] d_{min}: the minimum values of bonding length

[b] d_{avg}: average values of bonding length

Table S3 Integral quantity of Lewis acid sites of reduced catalysts.

Catalysts	Lewis acid sites [a] ($\mu mol \cdot g^{-1}$)	L/Pt (mol/mol)
0.5Pt1Sn/SiO_2	21.25	1.76
0.5Pt1Sn/N-SiO_2	14.04	1.01
0.5Pt1Sn/NHSS	20.23	1.17

[a] Amount of adsorbed pyridine (integration regions: 1430-1470 cm^{-1}).

The ratio of L/Pt of all the catalysts were higher than 1 (Table S3), ensuring the enough Lewis acid sites for the activation of acetic acid. Thus, the dissociative adsorption of H_2 on exposed Pt active sites was the rate determination step and increased the surface exposed Pt sites can effectively accelerate the hydrogenation rate. The experiment results showed that the apparent activity of the catalysts was only dependent on the amount of exposed Pt active sites.